

# Comparison between conventional and inverted solar cells using open circuit voltage decay transients

Upkar K. Verma,<sup>1,2</sup> Sunil Kumar,<sup>1,2</sup> and Y. N. Mohapatra<sup>1,2,3</sup>

<sup>1</sup>Department of Physics, Indian Institute of Technology Kanpur, Kanpur 208016, India

<sup>2</sup>National Centre for Flexible Electronics, Indian Institute of Technology Kanpur, Kanpur 208016, India

<sup>3</sup>Materials Science Programme, Indian Institute of Technology Kanpur, Kanpur 208016, India

(Received 28 June 2017; accepted 15 August 2017; published online 30 August 2017)

In the development of new structures for solar cells, it has become important to extract the true ideality factor of a diode, disentangling it from other loss mechanisms in the device. We use the open circuit voltage decay (OCVD) transient to obtain ideality factors and isolate the internal loss mechanisms in P3HT:PCBM bulk heterojunction solar cells. We compare two different structures using OCVD transients over more than six orders in timescale. The equivalent circuit parameters of diodes can be reliably extracted from such decays. Specifically, the numerical solution of the transient allows the determination of the diode ideality factor, and the saturation leakage current. In addition, this technique makes it possible to determine the diode current in the presence of excess carriers under photo irradiance, and hence, the light induced recombination current and shunt resistance can be separately extracted. We compare the decay transients of an efficient device with a leaky device and demonstrate that the diode current changes in the same manner in both the cases. We study in detail the intensity power-law dependence of the recombination current that controls the decay transient and observe that it increases significantly faster in leaky devices with light intensity. *Published by AIP Publishing.* [<http://dx.doi.org/10.1063/1.4993274>]

## I. INTRODUCTION

The blends of polymers and fullerene derivatives, specially Poly(3-hexylthiophene-2,5-diyl):Phenyl-C61-butyric acid methyl ester (P3HT:PCBM) systems, have served as a model material system in the field of organic solar cells.<sup>1–4</sup> Intensive studies are being carried out to push up the efficiency of the solar cells by modifying the device architecture and understanding the underlying mechanisms.<sup>5–12</sup> However, the intrinsic recombination loss processes have not been understood adequately in order to distinguish between Shockley-Reed-Hall (SRH), bimolecular, or geminate recombination mechanisms operative in the test structures.<sup>4,13</sup> Many conflicting interpretations have been made while isolating dominant loss mechanisms using various techniques such as steady state,<sup>8,14,15</sup> transient,<sup>16,17</sup> and impedance spectroscopy.<sup>18–21</sup> The main aim of these studies has been to estimate the order of reaction which is indicative of the dominant recombination mechanism.<sup>22–24</sup> However a coherent understanding of the recombination processes is yet to emerge specially for the differences under short circuit condition, operational bias, and open circuit condition.<sup>3</sup> Therefore, it becomes important to investigate the recombination losses under different bias conditions and understand the governing loss mechanisms.

A key to such studies is to have a reasonable equivalent circuit model of the device such that the components of current are clearly identified and isolated. The parameters such as ideality factor, the shunt, and the series resistance have been estimated by modeling the steady state current density-voltage (J-V) characteristics using equivalent circuit models under dark and white light illumination, and their dependence on the illumination intensity has been demonstrated.<sup>25,26</sup> However, modeling the transport characteristics such as J-V often

involve the contributions from multiple mechanisms; hence, the true estimation of reaction order becomes difficult under illumination. Recently, attempts have been made to understand the order of the reaction and relate it to the recombination losses.<sup>10,23</sup> The ideality factor has been defined in many different ways in order to interpret the governing loss mechanisms.<sup>10,27,28</sup> A significant strategy is to understand open circuit voltage since it completely avoids transport (e.g., the need to monitor series resistance) and focus on recombination mechanism alone. The intensity dependence of open circuit voltage ( $V_{OC}$ ) is typically investigated to identify the nature of the nongeminate recombination.<sup>27,29</sup>

In the past few years, transient techniques such as transient photo-voltage (TPV)<sup>10,30,31</sup> have also been used to isolate the recombination mechanisms. The TPV response has been modeled using exponential decay where the characteristic time constant is supposed to yield the carrier life time. By considering the recombination process to be monomolecular, i.e., trap assisted and using the SRH recombination mechanism, the carrier lifetime is related to the density of the localized states present in the HOMO-LUMO gap responsible for the recombination.<sup>32,33</sup> However, there is growing evidence that it would be an oversimplification to consider the recombination process to be monomolecular only. Moreover, it has always been a matter of debate in the literature whether the modeling of the TPV can yield the carrier lifetime.<sup>34</sup> The lack of a comprehensive model can lead to serious interpretational difficulties in the modeling of TPV characteristics and the associated loss mechanisms.

Furthermore, it is important to distinguish between the charge processes occurring in presence of light and under dark condition. This can be conventionally accomplished

through open circuit voltage decay (OCVD) transients. Recently, Rao *et al.*<sup>35</sup> have demonstrated that the OCVD transients of a specifically optimized solar cell with minimal leakage can be modeled using a circuit containing diode coupled with a capacitor. They have ignored the effect of dark shunt resistance as it was very high in the test structure used as a demonstration in their study. However, in practical devices the dark shunt resistance is of finite value and contributes to the shunt current which plays a crucial role in determining the device characteristics. Therefore, the current through the shunt resistance needs to be taken into account while modeling the OCVD characteristics in order to make the method more robust and routinely applicable to practical devices.

In this paper, we demonstrate that the OCVD transients of typical solar cells can be modeled in the whole measured range of time using an equivalent circuit containing a diode coupled with a capacitor and a resistor in parallel. The addition of the resistor makes the technique more general and useful than proposed before,<sup>35</sup> and it can be applied even to a leaky device with low shunt resistance. This provides a very reliable way of estimating true ideality factor of the diode in structures in which the shunt current can be significant. Consideration of dark leakage current is specifically important in the process of development of organic solar cells especially with a new process or substrate such as plastic, metal film, or paper. We estimate the shunt current generated due to the recombination of excess photo-generated charge carriers in the presence of white light and corresponding shunt resistance as a function of light intensity. This method gives an opportunity to get an insight into the dominant recombination pathways in a solar cell under white light illumination. A comparison between the two architectures keeping all other conditions same can help isolate bulk and contact related limitations. Further, there has been a growing interest<sup>36–38</sup> in architectures in which the bottom illumination layer becomes the cathode instead of using PEDOT:PSS as the anode. We compare the conventional structure with the inverted structure using OCVD transients, by extracting the functional dependence of different current components, and the associated circuit parameters. We demonstrate that the technique of OCVD can be used reliably even for devices with relatively low efficiencies so that it can be extended to flexible solar cells currently under development.

## II. EXPERIMENTAL DETAILS

In this paper, we use P3HT:PCBM based conventional as well as inverted bulk heterojunction (BHJ) solar cells having the structures ITO|PEDOT:PSS|P3HT:PCBM|Al and ITO|ZnO|P3HT:PCBM|MoO<sub>3</sub>|Ag, respectively. In the later structure, the illumination is through the cathode, and hence, it is referred to as the inverted structure. The inverted structure is a good quality device having low leakage current and higher power conversion efficiency while the conventional structure is a shunt limited leaky device with relatively lower efficiency. We deliberately choose the leaky device so as to demonstrate the robustness of the technique.

The organic materials poly(3-hexylthiophene) (P3HT) and phenyl-C61-butyric acid methyl ester (PCBM), used in

active layer formation, were procured from Sigma Aldrich. The commercial source Clevios provided the polymer Poly(3,4-ethylenedioxythiophene): polystyrene sulfonate (PEDOT:PSS). The fabrication of conventional BHJ solar cell is a multistep process. At first, a hole transporting layer of PEDOT:PSS is spin coated on the ITO coated glass substrates of desired pattern and subsequently annealed at 120 °C for 20 min on a hot plate resulting in a thickness of approximately 35 nm. In the next step, the active layer of P3HT:PCBM is formed by spin coating the blend solution of P3HT and PCBM mixed in a weight ratio of 1:1 in Chlorobenzene. The film is annealed at 140 °C for 20 min in nitrogen ambience on a hot plate and the resulting film thickness is measured to be approximately 100 nm. Thereafter, aluminum (Al) cathode is deposited thermally in high vacuum up to a thickness of 100 nm.

For the fabrication of inverted structure, a 30 nm thick electron transporting layer of zinc oxide (ZnO) is spin coated on patterned substrates of ITO coated glass and annealed at 250 °C for 10 min in air using a hot plate. Subsequently, the active layer of P3HT:PCBM is formed using the above mentioned process. Finally, Molybdenum trioxide (MoO<sub>3</sub>) and silver (Ag) were sequentially deposited via thermal evaporation in high vacuum up to the thicknesses of 5 and 100 nm, respectively. The sol-gel method is used to prepare ZnO solution with the ingredients zinc acetate dihydrate, monoethanolamine, and 2-methoxy ethanol. In this process, 4.895 ml 2-methoxy ethanol is used to dissolve 0.384 gm zinc acetate dihydrate with a subsequent addition of 0.105 ml of monoethanolamine. The overnight stirring of the solution is carried before processing. Keithley 2601 source measure unit and Agilent 4294 A impedance analyzer are used to measure J-V and C-V characteristics, respectively.

## III. RESULTS AND DISCUSSION

### A. Current density-voltage characteristics

Figure 1 shows the current density-voltage (J-V) characteristics of inverted and conventional solar cell structures both under dark and 1 sun illumination conditions on a semi-log scale. Both the structures are rectifying in nature with a rectification ratio of 4 orders of magnitude in the inverted structure, and 3 orders of magnitude in the case of conventional structure. The dark J-V characteristics, in both cases, exhibit three distinct regimes of current rise in the forward bias. At first, the current increases linearly in low bias range, and then follows an exponential rise in the mid-bias range, and eventually enters into the space charge limited (SCL) regime in deep bias. For a standard solar cell, the current density under dark condition is governed by Shockley diode equation neglecting the effect of shunt and series resistance as

$$J = J_o \left[ \exp \left( \frac{qV}{n_d k_B T} \right) - 1 \right], \quad (1)$$

where  $V$  is the applied voltage,  $q$  is elementary charge,  $n_d$  is the ideality factor,<sup>39</sup>  $k_B$  is the Boltzmann constant,  $T$  is the absolute temperature,  $J_o$  is the reverse saturation current density, and  $J$  is the current density at an applied voltage  $V$ . The

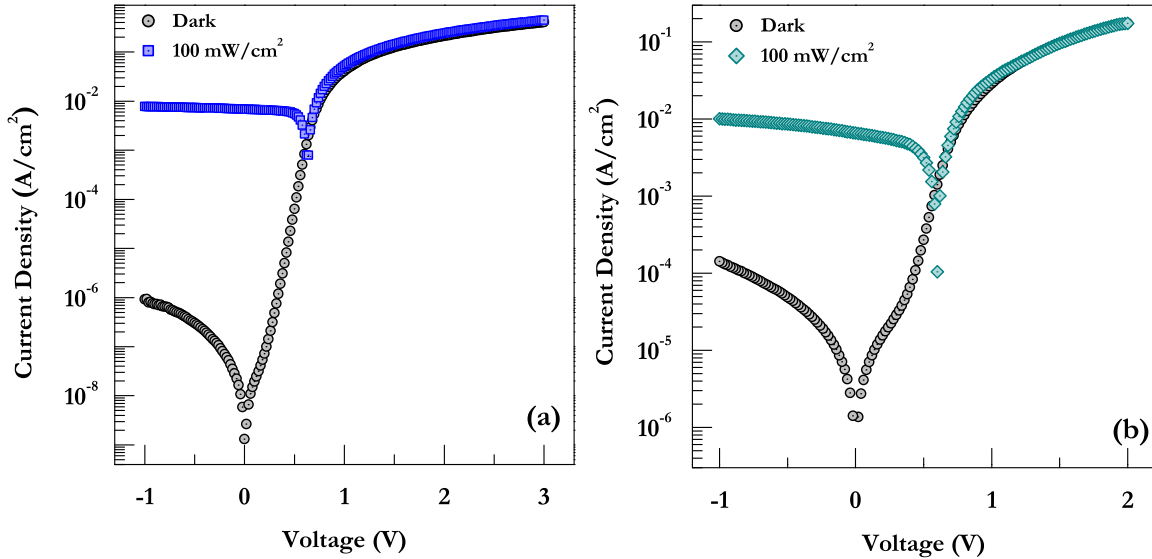


FIG. 1. J-V characteristics of (a) *inverted* (b) *conventional solar cell* structure under dark and illumination conditions on a semi-log scale.

ideality factors ( $n_d$ ) estimated applying Eq. (1) to the dark J-V characteristics are found to be 1.52 and 2.35 for inverted and conventional structures, respectively. The corresponding J-V characteristics under the illumination of 1 sun are also shown in Fig. 1 and the associated solar cell parameters are listed in Table I.

### B. Intensity dependence of open circuit voltage

The open circuit voltage ( $V_{OC}$ ) increases linearly with the natural logarithm of the illumination intensity. The functional dependence is as follows:<sup>27</sup>

$$V_{OC} = \frac{n_l k_B T}{q} \ln(\varphi), \quad (2)$$

where  $n_l$  is ideality factor,<sup>39</sup>  $k_B$  is the Boltzmann constant,  $T$  is the absolute temperature,  $q$  is the elementary charge, and  $\varphi$  being the intensity of illumination. Hence, the ideality factor  $n_l$  can be obtained from the slope of the  $V_{OC}$  vs.  $\ln(\varphi)$  curve.

The open circuit voltage ( $V_{OC}$ ) as a function of light intensity for the inverted and conventional structures is demonstrated in Fig. 2. The values of the ideality factor estimated from the slope of the curves come out to be 1.79 and 2.41 for

TABLE I. The parameters derived from J-V characteristics under dark and illumination and from intensity dependence of open circuit voltage for conventional and inverted solar cell structure.

Parameters	Conventional structure	Inverted structure
$V_{OC}$	0.60 V	0.64 V
$J_{SC}$	5.67 mA/cm <sup>2</sup>	6.58 mA/cm <sup>2</sup>
FF	0.55	0.65
Efficiency	1.87	2.78
$R_S$ (from J-V at one sun)	24.16 Ωcm <sup>2</sup>	22.06 Ωcm <sup>2</sup>
$R_{SH}$ (from J-V at one sun)	262 Ωcm <sup>2</sup>	920 Ωcm <sup>2</sup>
Ideality Factor ( $n_d$ ) (from dark J-V)	2.35	1.52
Ideality Factor ( $n_l$ ) (from $V_{OC}$ vs. $\ln \varphi$ )	1.79	2.41

inverted and conventional structures, respectively. A higher value of ideality factor indicates the dominance of recombination in the conventional structure. Usually, the ideality factor lies between 1 and 2 in case of organic solar cells, though sometimes it is found to be more than 2. Recently, it has been demonstrated that the ideality factor can be more than 2 depending upon the topology of the P3HT:PCBM blend.<sup>22</sup> In this case, though contact related non-idealities could be responsible for extra recombination currents as discussed later.

### C. Open circuit voltage decay transients

Figure 3 demonstrates the OCVD transient characteristics of a relatively more efficient inverted structure at an

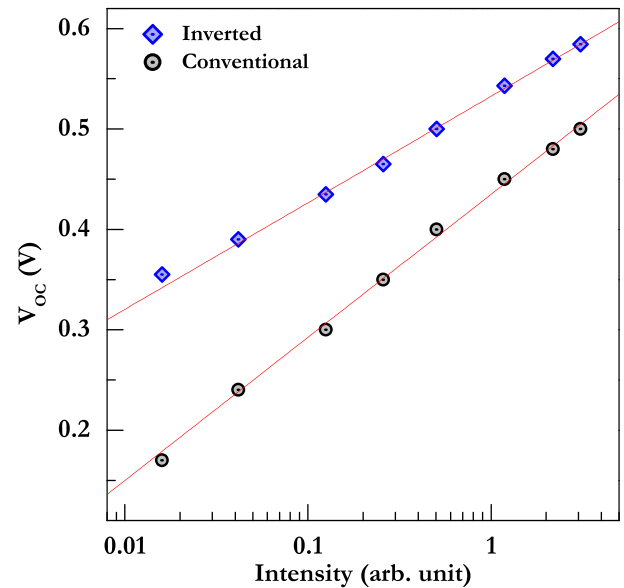


FIG. 2. Open circuit voltage of *conventional* and *inverted* solar cell structures as a function of illumination intensity. Note that it varies linearly with logarithm of illumination intensity.

arbitrary intensity plotted on a linear-log scale. It extends almost up to 10 s and recorded over 8 orders of magnitude in time starting from few nanoseconds. The characteristic curve exhibits three regimes of  $V_{OC}$  decay in logarithmic scale of time. At first, it is constant up to a certain time, then decays linearly with  $\log(t)$  and eventually goes to zero at last. The decay is successfully modeled using a circuit equivalent of the device as explained later, and the relevant parameters have been derived.

As shown in Fig. 3, in case of less efficient conventional structure also the decay characteristics are similar except that the decay is faster and lasts only up to few milliseconds. The time range up to which the  $V_{OC}$  decay curve is constant is almost the same in both the cases as can be seen from Fig. 3. However, the slope of the linear decay regime is higher in this case as compared to the inverted structure. The decay regime is controlled by the shunt resistance which is lower in conventional structure; hence, the decay is faster in this case. It is interesting to note that it is perhaps possible to estimate the true bulk lifetime of the photocarriers conveniently from the period during which  $V_{OC}$  remains constant in these decay curves.

#### D. Equivalent circuit of the device

Figure 4 shows the equivalent circuit of the test structures under dark condition. The effect of dark shunt has also been taken into account as evident from the figure. The series resistance ( $R_S$ ) has no role to play in open circuit condition as there will be no current flowing across it. The total current, i.e., the sum of the current flowing through the shunt resistance ( $I_{SH}$ ), diode current ( $I_D$ ), and the displacement current across the capacitor ( $I_d$ ), will be zero under open circuit condition. Therefore, at open circuit condition

$$I_D + I_{SH} + I_d = 0, \quad (3)$$

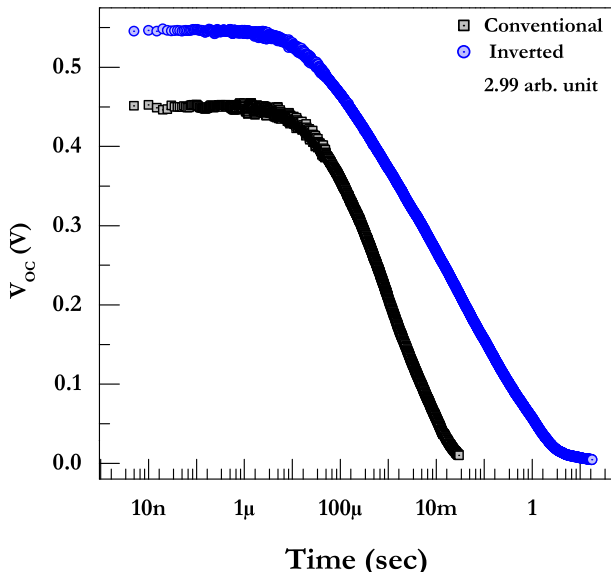


FIG. 3. OCVD transient characteristics of *conventional* and *inverted* solar cell structures at an arbitrary intensity of 2.99 arb. unit obtained by setting 15 mA current in the LED.

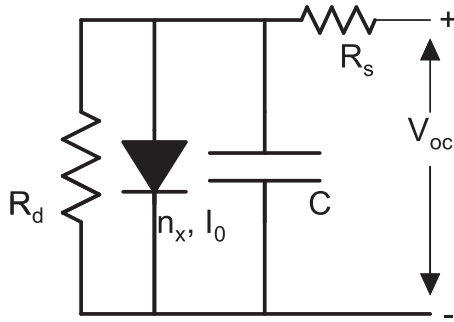


FIG. 4. The schematic diagram of the equivalent circuit of device under dark condition.

$$I_0 \left[ \exp \left( \frac{qV_{OC}}{n_X k_B T} \right) - 1 \right] + \frac{V_{OC}}{R_d} - C \frac{dV_{OC}}{dt} = 0, \quad (4)$$

where  $I_0$  is the dark saturation current,  $n_X$  is the ideality factor,<sup>39</sup>  $T$  is absolute temperature,  $k_B$  is Boltzmann constant,  $q$  is the elementary charge,  $R_d$  is the shunt resistance under dark condition, and  $C$  being the geometrical capacitance.

Equation (4) is a transcendental differential equation of first order, which can be solved numerically. The analytical solution can be obtained only in case we omit the shunt current term as shown previously.<sup>35</sup> We solve it in MATLAB using Runge Kutta method of solving numerical differential equation of first order. The experimental data are fitted with the numerical solution of Eq. (4) taking  $I_0$ ,  $n_X$ , and  $R_d$  as fitting parameters. The value of geometrical capacitance used in this computation is obtained from the capacitance-voltage characteristics in deep reverse bias.<sup>40</sup>

Under illumination, the light induced shunt resistance also comes into the picture as demonstrated in Fig. 5. The effective shunt resistance under illumination condition will be a parallel combination of dark shunt resistance ( $R_d$ ) and the light induced shunt resistance ( $R_{shl}$ ). The excess photo-carrier recombination in the presence of white light can be obtained by estimating the shunt current under illumination. The shunt current or the recombination current can be obtained by subtracting the diode current from the photo current ( $I_{ph}$ ). Photo current under the steady state open circuit condition can be approximated to the short circuit current ( $I_{SC}$ ). The light induced shunt resistance can be due to the appearance of new paths of recombination

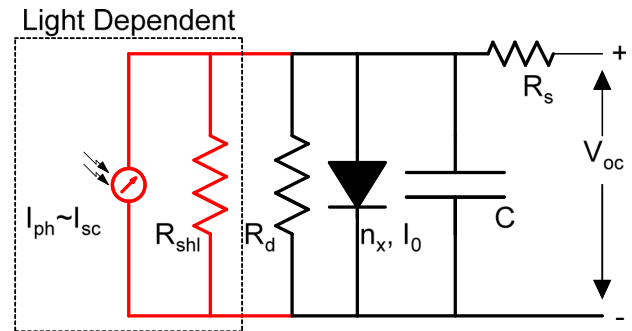


FIG. 5. The circuit equivalent of the test structure under light illumination. Note that the effective shunt resistance  $R_{SH}$  in this case is the parallel combination of the light induced shunt and the dark shunt resistance.

under illumination either at the interface or internal interfaces at the bulk junction without affecting the diode ideality factor.

## E. Modeling of open circuit voltage decay transients

### 1. For inverted structure

OCVD transient characteristics of an inverted solar cell structure are shown in Fig. 6 at various illumination intensities. The continuous (red) line indicates the fitting of the curves using Eq. (4). The capacitance value used in Eq. (4) is obtained from the capacitance-voltage measurements in deep reverse bias, which comes out to be 4.2 nF. The saturation current, dark shunt resistance and the ideality factor of the diode were the fitting parameters and estimated at different intensities of illumination. Indeed, the fitting is excellent over a wide range of time at all the intensities as can be seen from Fig. 6. The value of the dark shunt resistance is constant for all the intensities and comes out to be  $1 \times 10^9 \Omega$ . The ideality factor of the diode and the saturation current estimated from the modeling of the OCVD characteristics are listed in Table II for different illumination intensities. The dark reverse saturation current ranges from 56 to 60 pA which is nearly the same whereas the ideality factor increases with increasing intensity.

### 2. For conventional structure

For comparison, we now take up conventional structure, which is more leakier than the inverted structure. Figure 7 demonstrates the OCVD transients at various intensities of illumination in which the continuous (red) line indicates the fitting of the curves using the same equivalent model described by Eq. (4). The capacitance value in this case is estimated to be 5.66 nF from the capacitance-voltage characteristics in deep reverse bias. The modeling of the OCVD

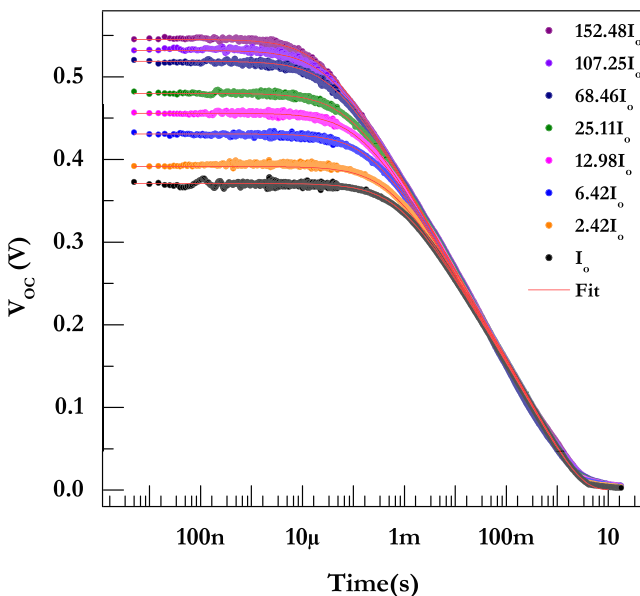


FIG. 6. OCVD transient characteristics of *inverted structure* at various illumination intensities fitted using the equivalent circuit model. Note that the continuous line denotes the fitting of OCVD curves and  $I_o$  is an arbitrary intensity whose value is 0.02 in terms of arbitrary units.

TABLE II. The ideality factor and saturation current under dark ( $I_o$ ) at different illumination intensities for *inverted structure* obtained by modeling the OCVD transient characteristics.

Relative light intensity (arb. unit)	Ideality factor ( $n_x$ )	Saturation current ( $I_o$ ) (pA)
0.02	1.720	56.0
0.05	1.726	56.3
0.13	1.738	56.9
0.25	1.746	57.6
0.49	1.754	57.8
1.34	1.775	58.5
2.10	1.780	59.0
2.99	1.790	60.0

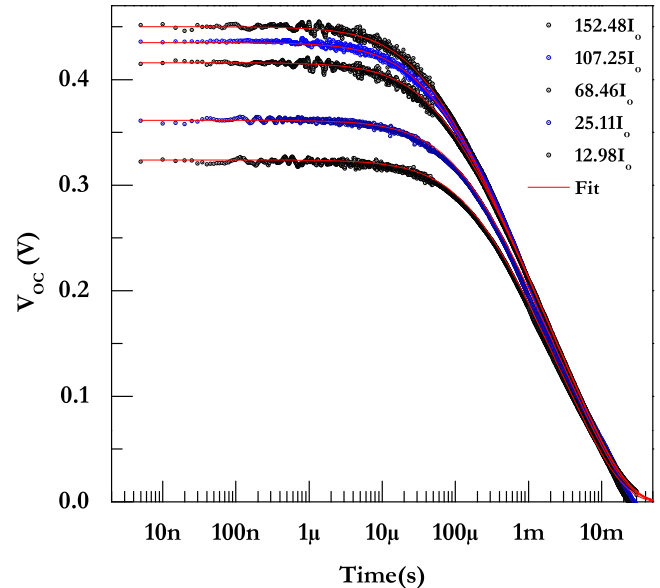


FIG. 7. OCVD transient characteristics of *conventional* leaky structure at various illumination intensities fitted using the equivalent circuit model.

characteristics using Eq. (4) yielded the value of dark shunt resistance to be  $5 \times 10^6 \Omega$  for all the curves recorded at different intensities. The dark saturation current lies between 21.80 nA to 17.00 nA, which is an insignificantly small variation for a pre-exponential term, and 3 orders of magnitude higher than the inverted structure. The ideality factor of the diode slightly increases with the enhancement in the illumination intensity as is evident from Table III. The ideality factor is higher in this case in comparison with the inverted structure, which implies that recombination is more in the

TABLE III. The ideality factor and saturation current under dark ( $I_o$ ) at different illumination intensities for *conventional structure* obtained by modeling the OCVD transient characteristics.

Relative light intensity (arb. unit)	Ideality factor ( $n_x$ )	Saturation current ( $I_o$ ) (nA)
0.25	2.687	21.80
0.49	2.687	18.50
1.34	2.687	16.65
2.10	2.688	16.75
2.99	2.690	17.00

present structure. We see that the analysis of OCVD transients allows the extraction of true parameters with unprecedented reliability and resolution.

## F. Loss mechanism at the open circuit condition

### 1. In inverted structure with low leakage

In the presence of light, the photo current ( $I_{ph}$ ) is divided into diode current ( $I_D$ ) and the shunt current ( $I_{SH}$ ). The shunt current in such a case is indicative of the recombination of the excess photo-generated charge carriers under illumination. We have already estimated the diode current at any bias from the modeling of OCVD transients. Further the photo current can be approximated to the short circuit current ( $I_{SC}$ ) under low injection condition at open circuit. Therefore, the shunt current under illumination can be obtained by subtracting the diode current from the short circuit current

$$I_{SH} = I_{ph} - I_{SC}. \quad (5)$$

The diode current, short circuit current, and the shunt current are shown as a function of intensity in Fig. 8 on log-log scale. As evident from Fig. 8, all the three currents increase with increasing intensity, exhibiting power-law behavior with the corresponding exponents being 0.70, 0.72, and 0.77, respectively. The shunt current is always less than the diode current in this structure. The value of the effective shunt resistance under illumination is calculated under steady state open circuit condition by taking the ratio of open circuit voltage to the shunt current in the presence of light. The shunt resistance under illumination also shows a power-law dependence on the illumination intensity as depicted in Fig. 11. The exponent for intensity dependence of shunt resistance is 0.69. The shunt resistance decreases with increasing intensity, which implies that the rate of

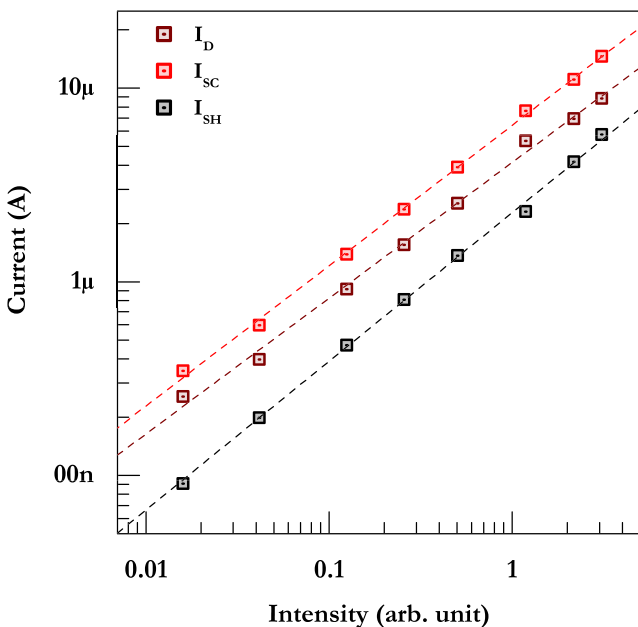


FIG. 8. The diode current ( $I_D$ ), short circuit current ( $I_{SC}$ ), and the recombination current in the presence of light ( $I_{SH}$ ) are shown as a function of intensity for *inverted structure* on a log-log scale.

recombination enhances with the increment in the concentration of photo-carriers.

### 2. In conventional leaky structure

The shunt current in the presence of light is obtained using Eq. (5) and plotted along with diode current and the short circuit current as exhibited in Fig. 10. The currents show a power-law dependence on the illumination intensity and the exponents for  $I_{SH}$ ,  $I_D$ , and  $I_{SC}$  are 1.10, 0.70, and 0.99, respectively. It can clearly be observed that the exponent for the diode current is same as in case of inverted structure. However, the exponent for  $I_{SH}$  is larger in this case and is more than unity. Figure 9 demonstrates that the shunt current is larger than the diode current throughout the measured range of the intensity except at very low intensity. Therefore, it is the shunt current that limits the device performance as the rate of recombination is higher in the present case of conventional structure.

## G. Comparison between the devices under test

A comparison between the parameters extracted from OCVD transients and different ideality factors estimated from dark J-V characteristics and light intensity dependence of  $V_{OC}$  is given in Table IV.

For the purposes of comparison of the light induced recombination current, Fig. 10 shows the shunt current as a function of intensity in the presence of light for both conventional as well as inverted structures. The shunt current in both the cases shows the power-law dependence upon the illumination intensity and the corresponding exponents are 1.10 and 0.77, respectively. Moreover, in conventional structure it increases sharply with increase in the intensity as compared to the inverted structure. The exponent in conventional structure

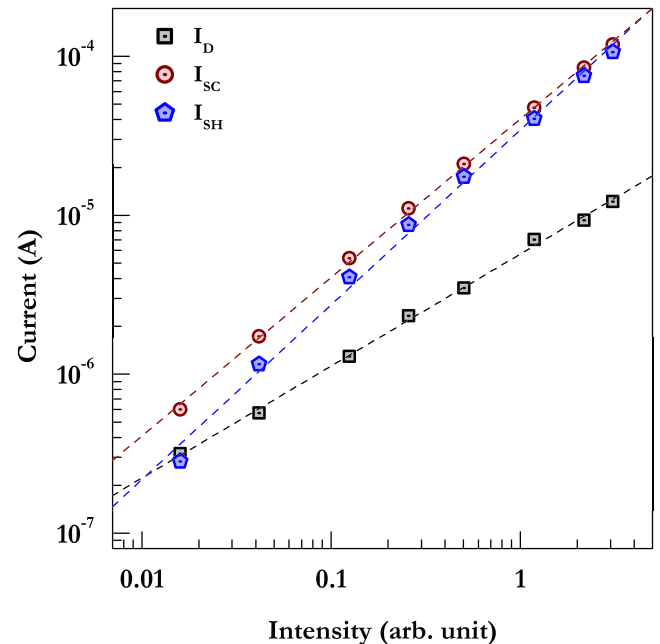


FIG. 9. The diode current ( $I_D$ ), short circuit current ( $I_{SC}$ ), and the recombination current in the presence of light ( $I_{SH}$ ) are shown as a function of intensity for *conventional structure* on a log-log scale.

TABLE IV. The parameters extracted for *conventional* and *inverted* solar cell structures.

Parameter	Conventional structure	Inverted structure
Ideality factor ( $n_x$ )	2.687–2.690	1.720–179
Ideality factor ( $n_l$ )	2.35	1.52
Ideality factor ( $n_d$ )	2.41	1.79
Saturation current ( $I_o$ )	21.80 nA–17.00 nA	56.0 pA–60.0 pA
Exponent for $I_D$	0.70	0.70
Exponent for $I_{SH}$	1.10	0.77
Exponent for $R_{SH}$	0.87	0.69

being greater than unity indicates that the device performance is limited by the shunt resistance to a greater extent.

We find that the effective shunt resistance as a function of light intensity is a good measure of comparison between two devices or structures. The effective shunt resistance in the presence of white light in both the cases exhibits power-law dependence with the intensity of illumination, and decreases with increasing intensity in both the structures as shown in Fig. 11. The corresponding exponents are found to be 0.87 and 0.69 for conventional and inverted structures, respectively. This shows that the functional dependence of effective shunt resistance under illumination is different, the conventional structure being significantly more leaky. Hence, it is the dark shunt resistance that controls the device characteristics and dominates the rate of the recombination even in the presence of light.

Also note that the shunt resistance ratio between the two structures increases with light intensity, i.e., the shunt current fraction rises more rapidly in the conventional structure. Since the active material is the same in both cases, it is the contacts that must be playing a role in bringing about the difference in the two cases. We have recently shown<sup>40</sup> that the

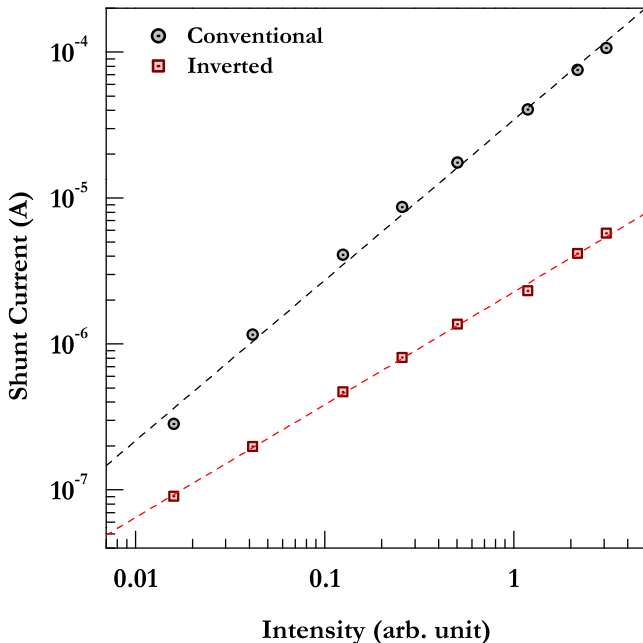


FIG. 10. Shunt current ( $I_{SH}$ ) is demonstrated as a function of intensity for both *conventional* and *inverted* structures.

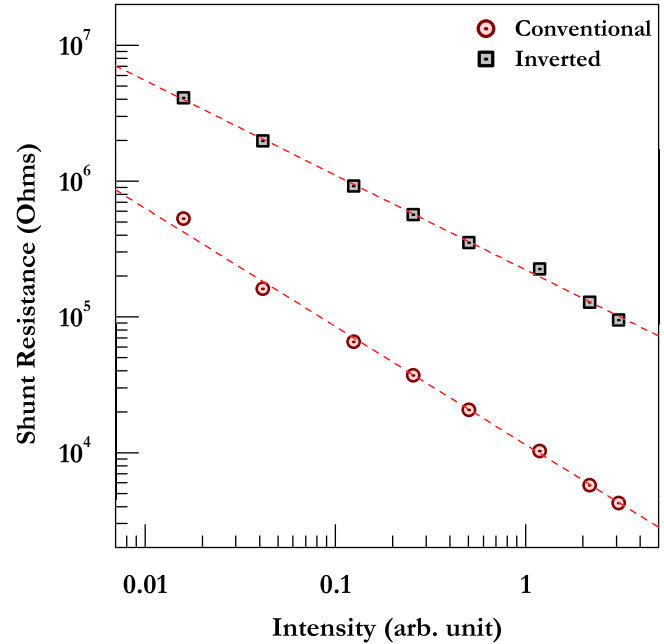


FIG. 11. Shunt resistance under illumination ( $R_{SH}$ ) is exhibited as a function of intensity for both *conventional* and *inverted* structures.

surface accumulation of carriers under light is significantly lower in the case of inverted structure. Hence, we conclude that recombination at the contacts and recombination in the bulk may be following different intensity dependence through carrier concentration. Therefore, it is reasonable to conclude that the net current and the associated exponents are significantly altered due to the contact or surface accumulation behavior. We have observed through our C-V analysis the presence of an additional barrier of 0.35 V in the conventional structure.<sup>40</sup>

The larger values of diode ideality factor for the conventional structure also points in the same direction. The ideality factor  $n_x$  extracted from OCVD transients is more representative than that of  $n_d$ , the diode ideality factor obtained from J-V characteristics, or  $n_l$ , i.e., obtained from the light intensity dependence of open circuit voltage. In any case, apart from  $n_x$ , all other parameters seem to be sensitive to the device architecture, including mechanisms operating at the contact. We believe that part of the confusion in the literature arises due to the comparison being made across devices and technology without explicitly taking into account the influence of the contact even in case of open circuit where the contact resistance has no role to play. This demonstrates the care that needs to be taken in comparing true bulk mechanisms.

#### IV. CONCLUSION

We have studied the open circuit voltage decay transients of P3HT:PCBM based inverted structure, having very high dark shunt resistance, with a leaky conventional structure having low shunt resistance under dark condition. The inclusion of dark shunt resistance makes the OCVD transient model applicable to a wide variety of practical solar cell structures. The transients have been modeled numerically

over a time span of almost eight orders of magnitude by using a combination of diode coupled with a capacitor and a resistor. The value of dark shunt resistance is  $1 \times 10^9 \Omega$  for inverted structure, while it is  $5 \times 10^6 \Omega$  in case of conventional leaky structure and the corresponding values of ideality factors extracted using the numerical model are found to vary with intensity of illumination between 1.72 to 1.79 and 2.68 to 2.69, respectively. The light induced recombination current and the shunt resistance exhibit a power law dependence on the illumination intensity, and the exponents were estimated to be 0.77 for low-leakage inverted structure, and 1.10 for conventional leaky structure with the corresponding exponents for light induced shunt resistance 0.69 and 0.87, respectively. The open circuit voltage decay transient is a powerful technique and can be used to estimate the shunt resistance under dark and illumination conditions. It provides a way to characterize the underlying recombination processes in a solar cell under operating conditions. Our results and analysis also clearly show the crucial importance of surface phenomena at the contacts even in open circuit conditions. The method can be easily extended to typically less efficient flexible solar cells on substrates such as plastic or paper currently under development using a variety of architectures and high speed printing methods.

## ACKNOWLEDGMENTS

This work was partially supported by Indo-German Science and Technology Centre through the Project FLEXIPRIDE [SCDT/IGSTC/20120009].

- <sup>1</sup>R. Ganesamoorthy, G. Sathiyan, and P. Sakthivel, *Sol. Energy Mater. Sol. Cells* **161**, 102 (2017).
- <sup>2</sup>L. Lu, T. Zheng, Q. Wu, A. M. Schneider, D. Zhao, and L. Yu, *Chem. Rev.* **115**, 12666 (2015).
- <sup>3</sup>L. Dou, J. You, Z. Hong, Z. Xu, G. Li, R. A. Street, and Y. Yang, *Adv. Mater.* **25**, 6642 (2013).
- <sup>4</sup>A. J. Heeger, *Adv. Mater.* **26**, 10 (2014).
- <sup>5</sup>S. Wood, D. O'Connor, C. W. Jones, J. D. Claverley, J. C. Blakesley, C. Giusca, and F. A. Castro, *Sol. Energy Mater. Sol. Cells* **161**, 89 (2017).
- <sup>6</sup>N. Tessler, *J. Appl. Phys.* **118**, 215501 (2015).
- <sup>7</sup>C. M. Proctor, M. Kuik, and T.-Q. Nguyen, *Prog. Polym. Sci.* **38**, 1941 (2013).
- <sup>8</sup>G. J. A. H. Wetzelar, N. J V d. Kaap, L. J. A. Koster, and P. W. M. Blom, *Adv. Energy Mater.* **3**, 1130 (2013).
- <sup>9</sup>T. Kirchartz and J. Nelson, in *Multiscale Modelling of Organic and Hybrid Photovoltaics*, edited by D. Beljonne and J. Cornil (Springer Berlin Heidelberg, Berlin, Heidelberg, 2014), p. 279.
- <sup>10</sup>A. Foertig, J. Rauh, V. Dyakonov, and C. Deibel, *Phys. Rev. B* **86**, 115302 (2012).
- <sup>11</sup>A. Rizzo, A. Cester, N. Wrachien, N. Lago, L. Torto, M. Barbato, J. Favaro, S. A. Gevorgyan, M. Corazza, and F. C. Krebs, *Sol. Energy Mater. Sol. Cells* **157**, 337 (2016).
- <sup>12</sup>F. C. Krebs and M. Jørgensen, *Adv. Opt. Mater.* **2**, 465 (2014).
- <sup>13</sup>A. Foertig, J. Kniepert, M. Gluecker, T. Brenner, V. Dyakonov, D. Neher, and C. Deibel, *Adv. Funct. Mater.* **24**, 1306 (2014).
- <sup>14</sup>S. Wheeler, F. Deledalle, N. Tokmoldin, T. Kirchartz, J. Nelson, and J. R. Durrant, *Phys. Rev. Appl.* **4**, 024020 (2015).
- <sup>15</sup>L. J. A. Koster, E. C. P. Smits, V. D. Mihailescu, and P. W. M. Blom, *Phys. Rev. B* **72**, 085205 (2005).
- <sup>16</sup>J. Kurpiers and D. Neher, *Sci. Rep.* **6**, 26832 (2016).
- <sup>17</sup>R. C. I. MacKenzie, C. G. Shuttle, M. L. Chabiny, and J. Nelson, *Adv. Energy Mater.* **2**, 662 (2012).
- <sup>18</sup>V. V. Brus, A. K. K. Kyaw, P. D. Maryanchuk, and J. Zhang, *Prog. Photovoltaics* **23**, 1526 (2015).
- <sup>19</sup>H. S. Duan, H. Zhou, Q. Chen, P. Sun, S. Luo, T. B. Song, B. Bob, and Y. Yang, *Phys. Chem. Chem. Phys.* **17**, 112 (2015).
- <sup>20</sup>B. Ray, A. G. Baradwaj, B. W. Boudouris, and M. A. Alam, *J. Phys. Chem. C* **118**, 17461 (2014).
- <sup>21</sup>H. Zang, Y. C. Hsiao, and B. Hu, *Phys. Chem. Chem. Phys.* **16**, 4971 (2014).
- <sup>22</sup>A. V. Nenashev, M. Wiemer, A. V. Dvurechenskii, F. Gebhard, M. Koch, and S. D. Baranovskii, *Appl. Phys. Lett.* **109**, 033301 (2016).
- <sup>23</sup>T. Kirchartz and J. Nelson, *Phys. Rev. B* **86**, 165201 (2012).
- <sup>24</sup>Y. Shi and X. Dong, *Phys. Chem. Chem. Phys.* **15**, 299 (2013).
- <sup>25</sup>B. Qi and J. Wang, *Phys. Chem. Chem. Phys.* **15**, 8972 (2013).
- <sup>26</sup>P. Kumar and S. Chand, *Prog. Photovoltaics* **20**, 377 (2012).
- <sup>27</sup>T. Kirchartz, F. Deledalle, P. S. Tuladhar, J. R. Durrant, and J. Nelson, *J. Phys. Chem. Lett.* **4**, 2371 (2013).
- <sup>28</sup>M. Soldera, K. Tarett, and T. Kirchartz, *Phys. Status Solidi A* **209**, 207 (2012).
- <sup>29</sup>N. K. Elumalai and A. Uddin, *Energy Environ. Sci.* **9**, 391 (2016).
- <sup>30</sup>D. Credgington and J. R. Durrant, *J. Phys. Chem. Lett.* **3**, 1465 (2012).
- <sup>31</sup>A. Baumann, K. Tvingstedt, M. C. Heiber, S. Väth, C. Momblona, H. J. Bolink, and V. Dyakonov, *APL Mater.* **2**, 081501 (2014).
- <sup>32</sup>A. K. Thakur, H. Baboz, G. Wantz, J. Hodgkiss, and L. Hirsch, *J. Appl. Phys.* **112**, 044502 (2012).
- <sup>33</sup>B. C. O'Regan, S. Scully, A. C. Mayer, E. Palomares, and J. Durrant, *J. Phys. Chem. B* **109**, 4616 (2005).
- <sup>34</sup>R. A. Street, *Phys. Rev. B* **84**, 075208 (2011).
- <sup>35</sup>K. S. Rao and Y. N. Mohapatra, *Appl. Phys. Lett.* **104**, 203303 (2014).
- <sup>36</sup>K. Wang, C. Liu, T. Meng, C. Yi, and X. Gong, *Chem. Soc. Rev.* **45**, 2937 (2016).
- <sup>37</sup>A. Savva, E. Georgiou, G. Papazoglou, A. Z. Chrusou, K. Kapnisis, and S. A. Choulis, *Sol. Energy Mater. Sol. Cells* **132**, 507 (2015).
- <sup>38</sup>Y.-J. Lee, B. L. Adkison, L. Xu, A. A. Kramer, and J. W. P. Hsu, *Sol. Energy Mater. Sol. Cells* **144**, 592 (2016).
- <sup>39</sup>In this paper, we distinguish between ideality factors obtained by different methods viz.  $n_d$  from J-V characteristics,  $n_i$  from intensity dependence of  $V_{oc}$ , and  $n_x$  from diode current as measured using OCVD transient.
- <sup>40</sup>U. K. Verma, S. Kumar, and Y. N. Mohapatra, *Sol. Energy Mater. Sol. Cells* **172**, 25 (2017).